06

To the theory of stimulated brillouine scattering in the field of 2D localized inhomogeneous pumping wave at an arbitrary scattering angle

© D.K. Solikhov[1], D.U. Hobilov[1], S.A. Dvinin[2]

[1] Tajik National University, Dushanbe, Tadjikistan
[2] Department of Physics, Moscow State University, Moscow, Russia

e-mail: davlat56@mail.ru

Received August 10, 2021
Revised December 12, 2021
Accepted December 25, 2021

The problem of stimulated Mandelstam-Brillouin scattering (SMBS) in a plasma in the field of a two-dimensionally localized and inhomogeneous pump wave is considered for arbitrary values ??of the scattering angle. Exact solutions of the system of truncated equations for the amplitude of an electromagnetic scattered wave and the amplitude of a sound wave are obtained in the approximation of strong dissipation of sound waves for an arbitrary direction of propagation of the scattered wave. The angular dependence of the intensity of the scattered radiation and its dependence on the inhomogeneity parameter of the pump wave are studied.

Keywords: stimulated Raman scattering: SRS, SBS, SBS, SRS, ionic sound, strong dissipation approach.

DOI: 10.21883/EOS.2022.04.53740.2631-21

Introduction

Stimulated Raman scattering (SRS) of light in a spatially-localized pumping wave field along one direction (flat layer) was discussed in many publications [1–3]. Absolute instability was reported for the localization region sizes exceeding a certain value which depends on the pumping wave amplitude. Such instability only occurs when the interacting wave group velocity projections on the pumping wave propagation direction are opposite in sign. Several modes are excited which differ in coordinate dependences of amplitude envelopes and have different thresholds and increments. Dependence of unstable wave amplitudes on coordinate was studied [1] and a single amplitude peak existing within the interaction region was reported for the first mode having the lowest threshold. Similar issues were discussed later regarding heterogeneous plasma [4]. Heterogeneous plasma generally means pumping wave heterogeneities.

Further development resulted in the study of parametric instabilities in two-dimensional geometry. Two-dimensionality occurs as a result of both plasma heterogeneity (limitation) and pumping wave field heterogeneity. Stimulated scattering in a 2D localized pumping wave filed in homogeneous plasma was discussed in many publications [5–8]. It was shown that exit of one of the waves beyond the interaction region boundary stabilizes absolute instability and convective wave amplification takes place when a specified threshold condition is satisfied. These findings are used in practice for plasma diagnostics, particle acceleration and interpretation of other nonlinear processes. In real experiments, medium is not always homogeneous and a question also arises regarding its influence on scattered radiation characteristics. Such issues were investigated in some early publications [9–13], but today they are getting of interest again due to new experimental results [14].

The scattering process is investigated herein using a reduced equation system for interacting wave amplitudes taking into account the medium heterogeneity [15]. An accurate solution for scattered emission intensity has been obtained and the dependence of the intensity on the scattering angle and typical pumping wave heterogeneity size at arbitrary scattering angles to a strong sound wave dissipation approximation (free path is much less lower than the heterogeneity size) has been studied.

Main equations

Consider a pumping wave with frequency ω_0 and wave vector $\mathbf{k}_0$ localized in a rectangular spatial region (Fig. 1) which propagates in the direction opposite to axis $0X$. The pumping wave and scattered wave interaction region is concentrated in rectangle $0 < y < L_2$, $-L_{1A} < x < L_{1B}$. Scattered wave vector projections (of sound and electromagnetic waves with frequencies ω_1, ω_2 and wave vectors $\mathbf{k}_1$ and $\mathbf{k}_2$) on axis $0X$ are of opposite sign. For the waves of interest, synchronism conditions $\omega_1 + \omega_2 = \omega_0$ are satisfied. Assume also that plasma heterogeneity or spatial configuration of the pumping wave result in the wave vector dependence of pumping wave $\mathbf{k}_0$, scattered sound wave $\mathbf{k}$ and scattered electromagnetic wave $\mathbf{k}_2$ on coordinate x. Due to this heterogeneity, wave vector synchronism conditions $\mathbf{k}_0 = \mathbf{k}_1 + \mathbf{k}_2$ are satisfied only at a certain coordinate value $x = x_0$. Without loss of generality, assume $x_0 = 0$.

To calculate instability development, specify the initial fluctuation whose evolution will later give birth to an instable mode. In a space-limited region, several methods

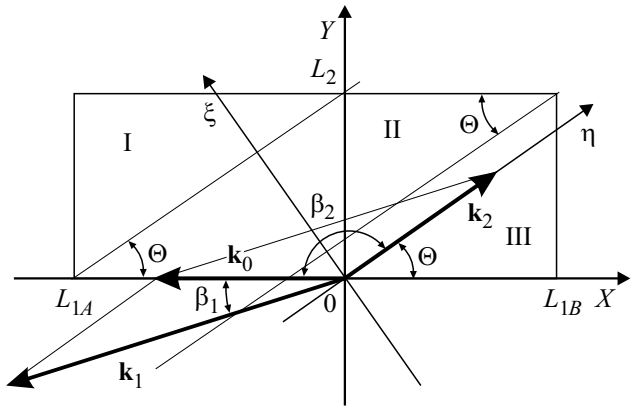

Figure 1. Wave vector interaction region and orientation ($\mathbf{k}_{0,1,2}$ are pumping wave, scattered sound and electromagnetic wave vectors, respectively).

may be used to specify the initial fluctuation. In an absolutely instable system, a local perturbation in the form of δ-function may serve as such fluctuation. Moreover, the width of this δ-function accommodates many wavelengths and this perturbation lasts longer than the lowest wave frequency in order to satisfy the synchronism conditions. Such approach is demonstrated in [16]. In an absolutely stable system, even when it is convectively instable, a space- and time-limited initial perturbation will give a time-limited response. Therefore, two approaches are usually addressed — response to a permanent perturbation (test wave) or response to repeatedly appearing and disappearing fluctuations. In the latter case, the system will generate a noise spectrum. At the initial (linear) instability development stage (threshold and increment calculation), all approaches lead to equations of the same type.

We assume herein that the initial perturbation is generated by a test electromagnetic wave propagating at an angle β_2 to axis $0X$. The sound wave propagates at an angle β_1 to axis $0X$. The equations for the interacting wave amplitudes a_1 and a_2 are as follows

$$\frac{\partial a_1}{\partial t} - V_s \cos\beta_1 \frac{\partial a_1}{\partial x} + V_s \sin\beta_1 \frac{\partial a_1}{\partial y} + \gamma_s a_1 = \nu_1 a_2 e^{-i\varphi(x)},$$

$$\frac{\partial a_2}{\partial t} + c\cos\beta_2 \frac{\partial a_2}{\partial x} - c\sin\beta_2 \frac{\partial a_2}{\partial y} + \gamma_t a_2 = \nu_2 a_1 e^{i\varphi(x)}, \tag{1}$$

where $a_1 = i\delta N/N_0$, δN is the electron concentration perturbation, $a_2 = \delta E^*$ is the scattered wave amplitude, V_s is the ion-sound wave velocity, c is the light velocity, $\gamma_{s,t}$ are sound and scattered wave damping factors, $\nu_{1,2}$ are nonlinear wave coupling coefficients proportional to the pumping wave amplitude. For Brillouin stimulated scattering processes (BSS), $\gamma_{s,t}$ and $\nu_{1,2}$ are defined as follows

$$\gamma_s = \frac{V_s^2}{2\omega_1}\frac{dk_{1x}(x)}{dx} + \frac{\nu_i}{2}, \quad \gamma_t = -\frac{1}{2}\frac{c^2}{\omega_2}\frac{dk_{2x}(x)}{dx} + \frac{\nu_e\omega_{Le}^2}{2\omega_2^2},$$

$$\nu_1 = \frac{Ze^2\varepsilon_0}{4mm_i}\frac{k_1}{\omega_0\omega_2 V_s}, \quad \nu_2 = \varepsilon_0^*\omega_{Le}^2/(4\omega_0),$$

where ν_i is the frequency of collision of ions with neutral particles or ions of other type, ν_2 is the frequency of collision of electrons with ions, e, m, N_0 is the electron charge, mass and concentration, Z, m_i is the charge number and mass of ions, ω_{Le} is the electron Langmuir frequency, ε_0 is the pumping wave amplitude which is considered as pre=defined, $\varphi(x) = \int_0^x \chi(x')dx'$ is the phase difference of scattered and sound waves interacting with the pumping wave due to plasma heterogeneity and pumping wave field, $\chi(x) = k_{0x}(x) - k_{2x}(x) - k_{1x}(x)$.

The equation system (1) applicable to BSS can be derived from microwave field plasma hydrodynamics equations and field equations [15,17]. To describe the scattering process, in addition to the angles β_1 and β_2, it is convenient to introduce also an angle $\theta = \pi - \beta_2$ (Fig. 1) which will be referred to as the scattering angle. For stimulated scattering processes, the angles β_1, β_2 and θ are not independent. For scattering with small variations of frequency ($\omega_1 \ll \omega_0$, $\omega_2 \cong \omega_0$), the wave vectors $\mathbf{k_0}$ and $\mathbf{k_2}$ have the same absolute values $k_2 \cong k_0$. This approximation is applicable when condition $\beta_2 \gg V_s/c$ is satisfied. Considering that $k_2 \cong k_0$, then $\beta_1 = (\pi - \beta_2)/2 = \theta/2$. The resonance wave interaction condition $\mathbf{k_0} = \mathbf{k_1} + \mathbf{k_2}$ means that $k_1 \approx 2k_0\sin(\theta/2) \approx 2k_0\cos(\beta_2/2)$.

For waves of opposite sign, group velocity projections on the directions of axes $0X$ and $0Y$, these angles vary within $\pi/2 \le \beta_2 \le \pi$, $0 \le \beta_1 \le \pi/4$, $0 \le \theta \le \pi$. Considering these, we obtain from (1)

$$-\cos\left(\frac{\theta}{2}\right)\frac{\partial a_1}{\partial x} - \sin\left(\frac{\theta}{2}\right)\frac{\partial a_1}{\partial y} + \gamma_1 a_1 = \mu_1 a_2 \cos\left(\frac{\theta}{2}\right) e^{-i\varphi(x)},$$

$$\cos\theta\frac{\partial a_2}{\partial x} + \sin\theta\frac{\partial a_2}{\partial y} + \gamma_2 a_2 = e^{-i\varphi(x)}, \tag{2}$$

where the following notations are introduced

$$\mu_1 = \frac{Ze^2\varepsilon_0}{2mm_i}\frac{k_0}{\omega_0^2 V_s^2}, \quad \mu_2 = \varepsilon_0^*\frac{\omega_{Le}^2}{4\omega_0 c},$$

$$\gamma_1 = \overline{\gamma}_s/V_s, \quad \gamma_2 = \overline{\gamma}_t/c.$$

$1/\overline{\gamma}_1 = V_s/\gamma_s$ determines the free path of the ion-sound wave, and $1/\overline{\gamma}_2 = c/\gamma_t$ determines the free path of the scattered wave. In view of the fact that a stationary process (response to a permanent perturbation) is addressed, time derivatives are omitted in (2).

Stimulated scattering at the angle $\theta = \pi/2$ (lateral scattering) and with other geometry in homogeneous plasma was addressed in [7]. For heterogeneous plasma, the lateral scattering in a 2D localized and heterogeneous pumping wave field was addressed recently in [18], and this research

is a follow-up of this publication for an arbitrary scattering angle.

Specify the boundary conditions in order to solve the problem. Assume that the high frequency wave amplitude a_2 in the point of entrance into the interaction region is constant, and the low frequency wave amplitude a_1 at the boundary is equal to zero:

$$a_1(x = L_{1B}, y) = a_1(x, y = L_2) = 0, \tag{3}$$

$$a_2(x, y = 0) = a_2(x = L_{1A}, y) = C. \tag{4}$$

Solution of equations (2) for zero boundary conditions enables to clear up the question about convective instability and to find amplification coefficients. In order to study spatial characteristics of the interacting wave amplitudes and angular dependence of scattered emission intensity, the equations (2) shall be solved with nonzero boundary conditions.

Spatial distribution of the scattered emission intensity with strong sound wave dissipation

Consider the solution of the equation system (2). In order avoid the phase factor, introduce new functions $b_{1,2}(x, y)$ as follows:

$$b_1(x, y) = a_1(x, y)\exp\big(i\varphi(x)/2\big),$$
$$b_2(x, y) = a_2(x, y)\exp\big(-i\varphi(x)/2\big). \tag{5}$$

Using (5), transform (2) to

$$-\cos\left(\frac{\theta}{2}\right)\frac{\partial b_1}{\partial x} - \sin\left(\frac{\theta}{2}\right)\frac{\partial b_1}{\partial y} + \left(\gamma_1 + \cos\left(\frac{\theta}{2}\right)\frac{i}{2}\chi(x)\right)b_1 = \mu_1\cos\left(\frac{\theta}{2}\right)b_2,$$

$$\cos\theta\frac{\partial b_2}{\partial x} + \sin\theta\frac{\partial b_2}{\partial y} + \left(\gamma_2 + \cos\theta\frac{i}{2}\chi(x)\right)b_2 = \mu_2 b_1. \tag{6}$$

Now, according to (3)–(5), the boundary conditions for function $b_{1,2}(x, y)$ will be as follows

$$b_1(x = L_{1B}, y) = b_1(x, y = L_2) = 0,$$
$$b_2(x = -L_{1A}, y) = C\exp\big(-i\varphi(-L_{1A})/2\big),$$
$$b_2(x, y = 0) = C\exp\big(-i\varphi(x)/2\big). \tag{7}$$

The scattering angle corresponds to the transition to lateral scattering $\theta = \pi/2$.

Consider solution (6) to a sufficiently strong sound wave damping approximation when derivatives $\partial b_1/\partial x(\partial y)$ may be ignored. $|\partial b_1/\partial x(\partial y)| \ll |\gamma_1, \chi|b_1$ is the approximation validity condition. The pumping wave field heterogeneity causes the wave interaction in plasma near the resonance point where the wave vector condition is satisfied ($\chi = 0$). Having chosen this point as the origin of coordinates, we can write in its neighborhood the following

$$\chi(x) = xk_0/L_0, \tag{8}$$

where L_0 is the scale of plasma or pumping wave heterogeneity. To a strong sound wave dissipation approximation, the equation (6) will be as follows

$$b_1 = \frac{\mu_1\cos(\theta/2)b_2}{\big(\gamma_1 + i\chi(x)\cos(\theta/2)/2\big)},$$

$$\cos\theta\frac{\partial b_2}{\partial x} + \sin\theta\frac{\partial b_2}{\partial y} + \left(\gamma_2 + \frac{i}{2}\cos\theta\chi(x) - \frac{\mu_2\mu_1\cos(\theta/2)}{\big(\gamma_1 + i\chi(x)\cos(\theta/2)/2\big)}\right)b_2 = 0. \tag{9}$$

Proceed to a new coordinate system, where

$$x = \eta\cos\theta + \xi\sin\theta, \quad y = \eta\sin\theta - \xi\cos\theta. \tag{10}$$

Inverse transformation is as follows

$$\eta = x\cos\theta + y\sin\theta, \quad \xi = x\sin\theta - y\cos\theta. \tag{11}$$

And the equation (8) reduces to:

$$\frac{1}{b_2}\frac{\partial b_2}{\partial\eta} = -\left(\gamma_2 + \frac{i}{2}\cos\theta\chi\big(x(\xi,\eta)\big) - \frac{\mu_2\mu_1\cos(\theta/2)}{\big(\gamma_1 + i\cos(\theta/2)\chi\big(x(\xi,\eta)\big)/2\big)}\right).$$

Thus, the equation contains a derivative with respect to only one coordinate (η), the second coordinate (ξ) is included in the equation only as a parameter. Along the wave propagation direction, $d\eta = dx/\cos\theta$ is satisfied. To achieve the result, divide the interaction region into two parts. When $-L_{1A} + y\,\mathrm{tg}(\theta) < x < L_{1B}$ (region I), the initial wave emission enters the region across the boundary $y = 0$, when the inverse condition is satisfied $-L_{1A} < x < -L_{1A} + y\,\mathrm{tg}(\theta)$ (region II) the initial wave emission enters the region across the boundary $x = L_{1B}$. Integration of the equation including the boundary conditions results in (here and below $\tilde{x}, \tilde{y}$ are the observation point coordinates, $\xi_1 = (\tilde{x}\sin\theta - \tilde{y}\cos\theta)$)

$$b_2(\tilde{x}, \tilde{y}) = b_2\Big(x_1\big(\xi(\tilde{x}, \tilde{y})\big), y_1\big(\xi(\tilde{x}, \tilde{y})\big)\Big)\exp\left(\int\limits_{x_1\left(\xi(\tilde{x},\tilde{y})\right)}^{\tilde{x}}\frac{dx'}{\cos\theta}\right.$$
$$\left.\times\left(\frac{\mu_2\mu_1\cos(\theta/2)}{\big(\gamma_1 + i\cos(\theta/2)\chi\big(x'(\xi,\eta)\big)/2\big)} - \gamma_2 - \frac{i}{2}\right.\right.$$
$$\left.\left.\times\cos\theta\chi\big(x'(\xi,\eta)\big)\right)\right).$$

Coordinate ξ is defined from coordinates $\tilde{x}, \tilde{y}$ of the observation point (where the field is calculated). The lower limit of integration x_1 — coordinate x of the point through which the scattered wave beam enters the scattering region is calculated using the following relations (Fig. 1):
in region I

$$\tilde{y} > (L_{1A} + \tilde{x}) \operatorname{tg}\theta, \quad x_1 = -L_{1A}, \tag{12}$$

and in regions II and III

$$\tilde{y} < (L_{1A} + \tilde{x}) \operatorname{tg}\theta, \quad x_1 = \tilde{x} - \tilde{y}/\operatorname{tg}\theta,$$
$$\tilde{y} > (L_{1A} + \tilde{x}) \operatorname{tg}\theta, \quad x_1 = -L_{1A}. \tag{13}$$

When $\theta \to \pi/2$, the integral remain finite because the distance between the integration points tends to zero. The scattered wave field amplitude $a_2(x, y)$ in the initial point is defined using relations (7), then we obtain

$$b_2(\tilde{x}, \tilde{y}) = C \exp\Big(-i\varphi\big(x_1(\tilde{x}, \tilde{y})\big)/2\Big) \exp\left(\int\limits_{x_1(\tilde{x},\tilde{y})}^{\tilde{x}} \frac{dx'}{\cos\theta} \right.$$
$$\times \left(\frac{\mu_2\mu_1 \cos(\theta/2)}{\Big(\gamma_1 + i\cos(\theta/2)\chi\big(x'(\xi,\eta)\big)/2\Big)} - \gamma_2 - \frac{i}{2} \right.$$
$$\left.\left. \times \cos\theta\chi\big(x'(\xi,\eta)\big) \right)\right).$$

The sound wave amplitude may be calculated as

$$b_1(\tilde{x}, \tilde{y}) = \mu_1 \cos(\theta/2) b_2(\tilde{x}, \tilde{y}) / \big(\gamma_1 + i\chi(\tilde{x})\cos(\theta/2)/2\big).$$

Finally, the equations (5) enable to obtain the final expression for the wave amplitudes in the interaction region (including the boundary):

$$a_2(\tilde{x}, \tilde{y}) = C \exp\Big(i\,\big(\varphi(\tilde{x}) - \varphi\big(x_1(\tilde{x}, \tilde{y})\big)\big)/2\Big)$$
$$\times \exp\left(\int\limits_{x_1(\tilde{x},\tilde{y})}^{\tilde{x}} \frac{dx'}{\cos\theta} \times \left(\frac{\mu_2\mu_1\cos(\theta/2)}{\Big(\gamma_1 + i\cos(\theta/2)\chi\big(x'(\xi,\eta)\big)/2\Big)} \right.\right.$$
$$\left.\left. - \gamma_2 - \frac{i}{2}\cos\theta\chi\big(x'(\xi,\eta)\big) \right)\right),$$
$$a_1(\tilde{x}, \tilde{y}) = \mu_1 a_2(\tilde{x}, \tilde{y}) / \big(\gamma_1 + i\chi(\tilde{x})\cos(\theta/2)/2\big)$$
$$\times \exp\big(-i\varphi(\tilde{x})\big). \tag{14}$$

Further simplification consists in the assumption that $\chi(\tilde{x})$ is rather monotonic therefore the linear approximation (8) may be used. Then

$$a_2(\tilde{x}, \tilde{y}) = C \exp\big(Q(\tilde{x}, x_1)/\cos\theta\big)$$
$$= C \exp\Big(\big(\Gamma(\tilde{x}) - \Gamma(x_1)\big)/\cos\theta\Big),$$
$$a_1(\tilde{x}, \tilde{y}) = \mu_1 \cos(\theta/2) a_2(\tilde{x}, \tilde{y}) / \big(\gamma_1$$
$$+ ik_0\cos(\theta/2)\tilde{x}/2L_0\big) \exp\big(-i\varphi(\tilde{x})\big), \tag{15}$$

$$\Gamma(x) = \left(-\gamma_2 L_2 \frac{x}{L_2} + \frac{2L_0\mu_2\mu_1}{k_0} \operatorname{arctg}\left(\frac{k_0 L_2}{2L_0\gamma_1} \frac{x}{L_2} \cos(\theta/2) \right) \right.$$
$$\left. - i\frac{L_0\mu_2\mu_1}{k_0} \ln\left(1 + \frac{k_0^2 L_2^2}{4\gamma_1^2 L_0^2} \frac{x^2}{L_2^2} \cos^2(\theta/2) \right) \right).$$

The last expression may be simplified by introducing the following dimensionless parameters: $A = 2L_0\gamma_1/k_0L_2$ which characterizes the relative role of wave heterogeneity and damping in plasma, $P = \mu_2\mu_1/\gamma_1\gamma_2$ which when $P = 1$, the intensity of the wave propagating along axis $0X$ in homogeneous medium remains unchanged). Having written the product of the wave amplification coefficient at convective instability in homogeneous medium and the lateral dimension L_2 at back scattering and underdamping of electromagnetic wave $G = \mu_2\mu_1 L_2/\gamma_1$, we obtain

$$\frac{\Gamma(x)}{\cos\theta} = \frac{G}{\cos\theta} \left(A \operatorname{arctg}\left(\frac{x}{AL_2} \cos(\theta/2) \right) - P^{-1} \frac{x}{L_2} \right.$$
$$\left. - i\frac{A}{2} \ln\left(1 + \frac{x^2}{A^2 L_2^2} \cos^2(\theta/2) \right) \right).$$

In a medium which is close to a homogeneous medium, $x\cos(\theta/2)/AL_2 \ll 1$, and the last equation is simplified:

$$\frac{\Gamma(x)}{\cos\theta} = \frac{G}{\cos\theta} \left(\big(\cos(\theta/2) - P^{-1}\big) \frac{x}{L_2} - i\frac{1}{2A} \frac{x^2}{L_2^2} \cos^2(\theta/2) \right). \tag{16}$$

In the limiting case of strong heterogeneity, $|x|\cos^2(\theta/2)/AL_2 \gg 1$, we have

$$\frac{\Gamma(x)}{\cos\theta} = \frac{G}{\cos\theta} \left(A\frac{\pi}{2}\operatorname{sign}(x) - P^{-1}\frac{x}{L_2} - i\frac{A}{2} \right.$$
$$\left. \times \ln\left(1 + \frac{x^2}{A^2 L_2^2} \cos^2(\theta/2) \right) \right).$$

Now obtain the final expressions for the wave amplitude.

At the boundary $y = L_2$ with $\tilde{x} < -L_{1A} + L_2 \operatorname{ctg}\theta$

$$\frac{Q(\tilde{x}, y = L_2)}{\cos\theta} = \frac{G}{\cos\theta} \left(A \left(\operatorname{arctg}\left(\frac{\tilde{x}}{AL_2} \cos(\theta/2) \right) \right.\right.$$
$$\left.\left. + \operatorname{arctg}\left(\frac{L_{1A}}{AL_2} \cos(\theta/2) \right) \right) - P^{-1}\left(\frac{\tilde{x}}{L_2} + \frac{L_{1A}}{L_2} \right) - i\frac{A}{2} \right.$$
$$\left. \times \ln\left(\left(1 + \frac{\tilde{x}^2}{A^2 L_2^2} \cos^2(\theta/2) \right) \Big/ \left(1 + \frac{L_{1A}^2}{A^2 L_2^2} \cos^2(\theta/2) \right) \right) \right), \tag{17}$$

at $\tilde{x} > -L_{1A} + L_2 \operatorname{ctg}\theta$

$$\frac{Q(\tilde{x}, y = L_2)}{\cos\theta} = \frac{G}{\cos\theta}\left(A\left(\operatorname{arctg}\left(\frac{\tilde{x}}{AL_2}\cos(\theta/2)\right)\right.\right.$$
$$\left.\left. - \operatorname{arctg}\left(\frac{\tilde{x} - L_2\operatorname{ctg}\theta}{AL_2}\cos(\theta/2)\right)\right)\right) - P^{-1}\operatorname{ctg}\theta - i\frac{A}{2}$$
$$\times \ln\left(\left(1+\frac{\tilde{x}^2}{A^2L_2^2}\cos^2(\theta/2)\right)\Big/\left(1+\frac{(\tilde{x} - L_2\operatorname{ctg}\theta)^2}{A^2L_2^2}\right.\right.$$
$$\left.\left.\times\cos^2(\theta/2)\right)\right), \tag{18}$$

At the boundary $x = L_{1B}$ with $y < (L_{1A} + L_{1B})\operatorname{tg}\theta$

$$\frac{Q(\tilde{x} = L_{1B}, y)}{\cos\theta} = \frac{G}{\cos\theta}\left(A\left(\operatorname{arctg}\left(\frac{L_{1B}}{AL_2}\cos(\theta/2)\right)\right.\right.$$
$$\left.\left. - \operatorname{arctg}\left(\frac{L_{1B} - y\operatorname{ctg}\theta}{AL_2}\cos(\theta/2)\right)\right)\right) - P^{-1}\frac{y\operatorname{tg}\theta}{L_2} - i\frac{A}{2}$$
$$\times \ln\left(\left(1+\frac{L_{1B}^2}{A^2L_2^2}\cos^2(\theta/2)\right)\Big/\left(1+\frac{(L_{1B} - y\operatorname{tg}\theta)^2}{A^2L_2^2}\right.\right.$$
$$\left.\left.\times\cos^2(\theta/2)\right)\right), \tag{19}$$

at $y > (L_{1A} + L_{1B})\operatorname{tg}\theta$

$$\frac{Q(\tilde{x} = L_{1B}, y)}{\cos\theta} = \frac{G}{\cos\theta}\left(A\left(\operatorname{arctg}\left(\frac{L_{1B}}{AL_2}\cos(\theta/2)\right)\right.\right.$$
$$\left.\left. + \operatorname{arctg}\left(\frac{L_{1A}}{AL_2}\cos(\theta/2)\right)\right)\right) - P^{-1}\frac{L_{1B} + L_{1A}}{L_2} - i\frac{A}{2}$$
$$\times \ln\left(\left(1+\frac{L_{1B}^2}{A^2L_2^2}\cos^2(\theta/2)\right)\Big/\left(1+\frac{L_{1A}^2}{A^2L_2^2}\right.\right.$$
$$\left.\left.\times\cos^2(\theta/2)\right)\right). \tag{20}$$

We will also give limits for expressions (18) and (19) when $\theta \to \pi/2$ which demonstrate the absence of singularity:

$$\frac{Q(\tilde{x}, y = L_2)}{\cos\theta} = G\left(\frac{\cos(\theta/2)}{\sin\theta}\Big/\left(1+\left(\frac{\tilde{x}}{AL_2}\cos(\theta/2)\right)^2\right)\right)$$
$$- \frac{\sin\theta}{P} - i\frac{A}{2}\frac{2\tilde{x}L_2\sin\theta}{A^2L_2^2}\cos^2(\theta/2)\Big/\left(1+\frac{\tilde{x}^2}{A^2L_2^2}\right.$$
$$\left.\times\cos^2(\theta/2)\right),$$

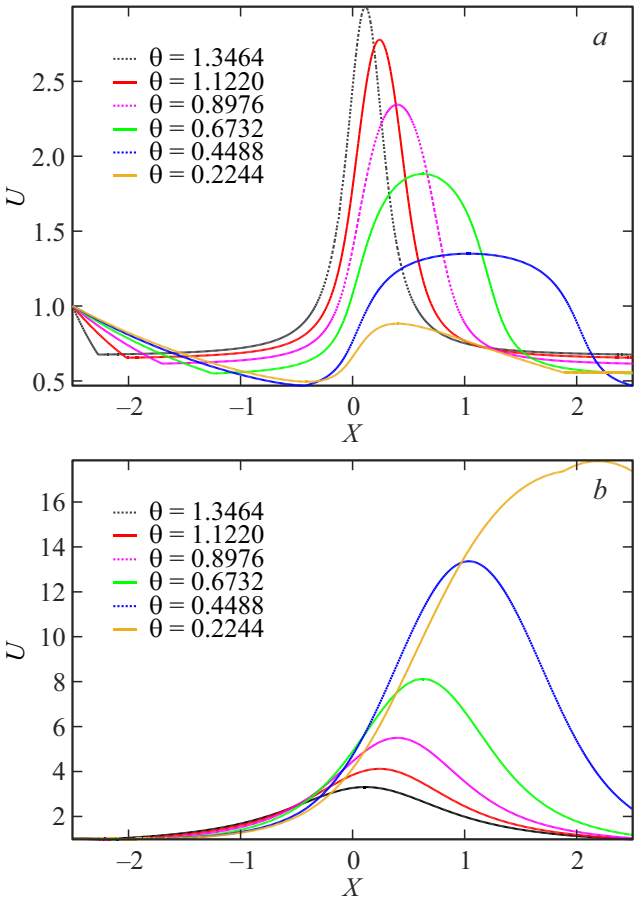

Figure 2. Wave amplification coefficient U vs. emission exit point, dimensionless heterogeneity length $A = 0.2$ (a), 1 (b); scattering region and pumping wave parameters $L_{1A}/L_2 = L_{1B}/L_2 = 2.5$, $X = x/L_2$, $P = 10$, $G = 1$.

$$\frac{Q(\tilde{x} = L_{1B}, y)}{\cos\theta} = G\left(\frac{y\cos(\theta/2)}{L_2\sin\theta}\Big/\left(1+\left(\frac{L_{1B}}{AL_2}\cos(\theta/2)\right)^2\right)\right)$$
$$- \frac{y}{PL_2\sin\theta} - i\frac{A}{2}\ln\left(\left(1+\frac{L_{1B}^2}{A^2L_2^2}\cos^2(\theta/2)\right)\right.$$
$$\left.\Big/\left(1+\frac{(L_{1B} - y\operatorname{tg}\theta)^2}{A^2L_2^2}\cos^2(\theta/2)\right)\right).$$

According to the obtained equations, the qualitative form of the obtained relations depends on the dimensionless parameters L_{1A}/L_2, L_{1B}/L_2 which characterize the system geometry, A the system heterogeneity, P the threshold crossing in a homogeneous infinite medium.

Parameter G, which determines the signal amplification, characterizes the curve range without affecting its qualitative behavior. The results of calculations of the dimensionless parameter $U(x, y) = Q(x, y = L_2)/G\cos\theta$ depending on the dimensionless coordinate of the emission exit point $X = x/L_2$ are shown in Fig. 2. For short characteristic heterogeneity lengths L_0. $(A < 1$, Fig. 2, $a)$, the scattered waves passing through point $x = 0$ on the symmetry line

$y = L_2/2$ are amplified as much as possible. For the angle θ close to $\pi/2$ (distance along axis $0Y$), the half-width of the coordinate region where scattering takes place is close to L_0. Reduced scattering angle caused the increase in the coordinate region where the amplification takes place, however, the scattered wave amplification decreases. Increased characteristic heterogeneity length (and coefficient A (Fig. 2, b, $A = 1$)) causes widening of the maximum amplification region and shifting of the maximum amplification towards the right boundary of the interaction region. Since the optical path covered by the beam in the field amplification region grows with the reduction of the angle θ, then the signal amplification also grows. For $A \gg 1$ when $L_2 < L_{1A} + L_{1B}$ is satisfied, the simplified equation (16) is valid, and the main emission portion exits through the boundary $x = L_{1B}$.

Breaks of the curves in Fig. 2 are associated with the test wave entrance through the boundary $x = -L_{1A}$ or the boundary $y = 0$. The squared absolute value of emission amplitude is expressed as follows

$$|a_2(\tilde{x}, \tilde{y})|^2 = C \exp(2\mathrm{Re}Q(\tilde{x}, \tilde{y})/\cos\theta). \qquad (21)$$

It should be noted that the angular dependence of the scattered wave intensity in a heterogeneous medium depends heavily on the amplification threshold crossing at the the given pumping wave amplitude. This is because of the fact that the wave propagating at small scattering angles θ passes consecutively the amplification region (near the origin of coordinates) and damping region (near the boundaries). Therefore, when the threshold is exceeded to a minor extent, the integral amplification may be suppressed due to absorption in the region where no interaction is present (Fig. 2, a). For low damping and large A, scattering at small angles is more intensive (Fig. 2, b).

It should be noted that since scattering is determined by several parameters with length dimension (L_0, L_{1A}, L_{1B}, L_2), the choice of dimensionless parameters A, G, P to describe the process is ambiguous. In some cases, $\tilde{A} = 2\gamma_1/k_0$ and $\tilde{G} = \mu_2\mu_1 L_0/\gamma_1$ may be more convenient. Then the expression for $\Gamma(x)$ will be as follows

$$\Gamma(x) = \tilde{G}\left(\tilde{A}\,\mathrm{arctg}\left(\tilde{A}^{-1}\frac{x}{L_0}\cos(\theta/2)\right) - P^{-1}\frac{x}{L_0} - 2i\tilde{A}\ln\left(1 + \tilde{A}^{-2}\frac{x^2}{L_0^2}\cos^2(\theta/2)\right)\right).$$

Scattered emission intensity calculation

The experimental study of BSS are focused on the scattered field intensity at the wave interaction region exit rather that on the scattered field amplitude [19–21]. According to the findings in the previous section, the

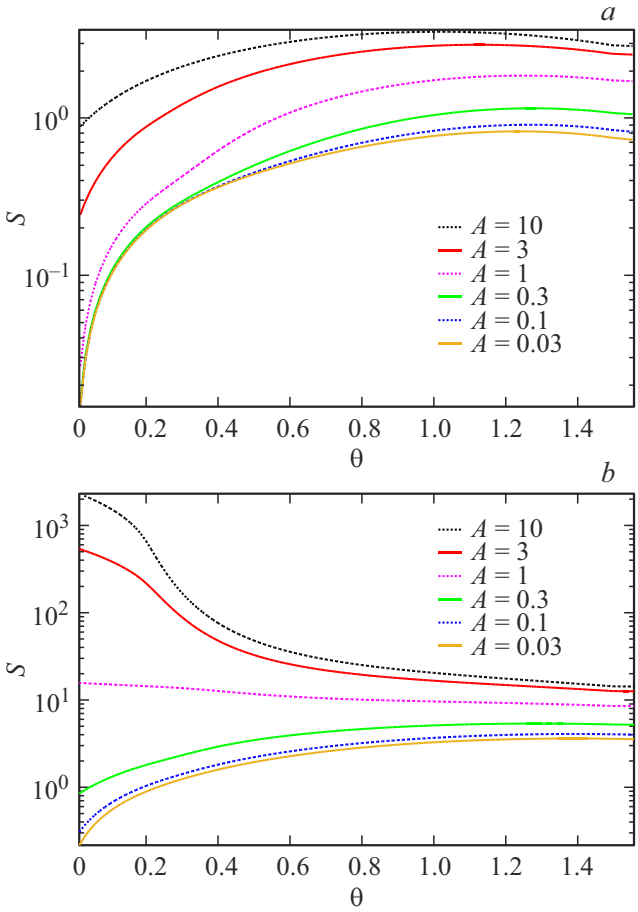

Figure 3. Scattered emission intensity S vs. scattering angle θ at different pumping wave heterogeneities A, spatial amplification coefficient in a homogeneous medium $G = 1$, instability threshold crossing in a homogeneous medium $P = 1$ (a), 5 (b), Scattering region dimensions $L_{1A}/L_2 = L_{1B}/L_2 = 2.5$.

scattered wave intensity is

$$I_S(\theta, L_0, L_{1A}, L_{1B}, L_2) = \left\{\int_{-L_{1A}}^{+L_{1B}} |a_2(x, y = L_2)|^2 \sin\theta dx + \int_0^{L_2} |a_2(x = L_{1B}, y)|^2 \cos\theta dy\right\}. \qquad (22)$$

By substituting (21) in (22), after integration ,we obtain the explicit form of the scattered emission intensity vs. the test wave intensity:

$$S(\theta, L_0, L_{1A}, L_{1B}, L_2) = I_S(\theta, L_0, L_{1A}, L_{1B}, L_2)/|C|^2.$$

At $L_2 < (L_{1B} + L_{1A})\,\mathrm{tg}\,\theta$

$$S(\theta, L_0, L_{1A}, L_{1B}, L_2) = \left\{ \int_{-L_{1A}}^{-L_{1A}+L_2\,\mathrm{ctg}\,\theta} \exp\Big(2\big(G(x) - G(-L_{1A})\big)\Big) \sin\theta dx + \int_{-L_{1A}+L_2\,\mathrm{ctg}\,\theta}^{-L_{1B}} \exp\Big(2\big(G(x) - G(x - L_2\,\mathrm{ctg}\,\theta)\big)\Big) \sin\theta dx + \int_{0}^{L_2} \exp\Big(2\big(G(L_{1B}) - G(L_{1B} - y\,\mathrm{ctg}\,\theta)\big)\Big) \cos\theta dy \right\}.$$

At $L_2 > (L_{1B} + L_{1A})\,\mathrm{tg}\,\theta$

$$S(\theta, L_0, L_{1A}, L_{1B}, L_2) = \left\{ \int_{-L_{1A}}^{L_{1B}} \exp\Big(2\big(G(x) - G(-L_{1A})\big)\Big) \times \sin\theta dx + \int_{0}^{(L_{1A}+L_{1B})\,\mathrm{tg}\,\theta} \exp\Big(2\big(G(L_{1B}) - G(L_{1B} - x\,\mathrm{ctg}\,\theta)\big)\Big) \cos\theta dy + \int_{(L_{1A}+L_{1B})\,\mathrm{tg}\,\theta}^{L_2} \exp\Big(2\big(G(L_{1B}) - G(L_{1A})\big)\Big) \cos\theta dy \right\}.$$

The calculation example for the scattered emission intensity as function of the scattering angle at different heterogeneity lengths is shown in Fig. 3. At low pumping wave intensities ($P = 1$, Fig. 3, *a*), the signal is attenuated higher than for propagation along axis $0X$ ($\theta \to 0$), and the degree of attenuation is determined by the amplification regions dimensions (L_0) vs. the total plasma length (L_{1A} and L_{1B}). Since ($L_{1A} + L_{1B} > L_2$), for propagation across the scattering region ($\theta \to \pi/2$), the signal attenuation at small A is lower and the test wave intensity amplification is observed at large A.

When the convective instability threshold is exceeded to a high extent ($P = 10$, Fig. 3, *b*) and dimensions L_0 and L_2 are close to each other, the angular dependence is very low. When $A < 1$, the scattered energy increases with the scattering angle, and when $A > 1$, it grows.

A similar calculation of the scattering intensity as function of coefficient A at several scattering angles is shown in Fig. 4. When the convective instability threshold is exceeded to a great extent, the emission intensity grows with an increase in the characteristic heterogeneity size. Curve saturation in Fig. 4 is associated with the fact that the characteristic heterogeneity size exceeds the interaction region size. As discussed above, when the threshold is exceeded to a low extent, electromagnetic wave damping plays a significant role causing qualitative change in the angular dependence of the scattered emission.

Either the scattered emission power I_S vs. the pumping wave power I_0, $W_1 = I_S/I_0$ at the pre-defined test wave amplitude I_2, or the power I_S vs. the test wave power I_2 at the pre-defined I_0, $W_1 = I_S/I_0$ is of physical significance. The pumping wave intensity is

$$I_0 = |\varepsilon_0|^2 L_2,$$

and the test wave intensity is

$$I_2 = |C|^2 (L_2 \cos\theta + (L_{1A} + L_{1B}) \sin\theta).$$

To assess the applicability of the findings, we will show the results of the experiments with laser emission BSS. In experimental conditions [21], where laser emission BSS was studied in low-density gas target plasma with the following parameters $\omega_{Le} = (3.1{-}8.9) \cdot 10^{13}\,\mathrm{s}^{-1}$, $\omega_0 = 2 \cdot 10^{14}\,\mathrm{s}^{-1}$ (CO_2-laser) $\to \lambda_0 \cong 10^{-3}$ cm, $T_e = 50 - 100$ eV energy flux density in a beam, $p = (10^{11}{-}10^{13})\,\mathrm{W/cm}^2$; $V_e/V_{Te} \cong 0.3$, the instability threshold $P = 1$ is achieved at the energy flux density $p_{\mathrm{limit}} = (1.5 \cdot 10^8 \div 2.6 \cdot 10^{10})\,\mathrm{W/cm}^2$, and amplification coefficient $q = G/L_2$ is calculated as $G/L_2 \cong (4.5 \cdot 10^2 \div 4.2 \cdot 10^3)\,\mathrm{cm}^{-1}$. Since in these experiments $p > p_{\mathrm{limit}}$, then the scattered emission growth as $\exp(qx)$ shall be expected, where the maximum x is determined by the acoustics length and is equal to $L_1 = \lambda_0 (L_2/2\lambda_0)^2 \cong (1.6 \cdot 10^{-2} \div 10)$ cm and $G \cong (7.2 \div 4.2 \cdot 10^4)$.

In our numerical calculations, q is equal to $\approx 2 \cdot 10^2\,\mathrm{cm}^{-1}$. Hence, the wave amplification coefficients coincide by the order of magnitude. If the experimental value is assumed for L_1, then we obtain $G(L_{1A} + L_{1B})/L_2 \cong (3.2{-}2 \cdot 10^3)$, which almost coincides

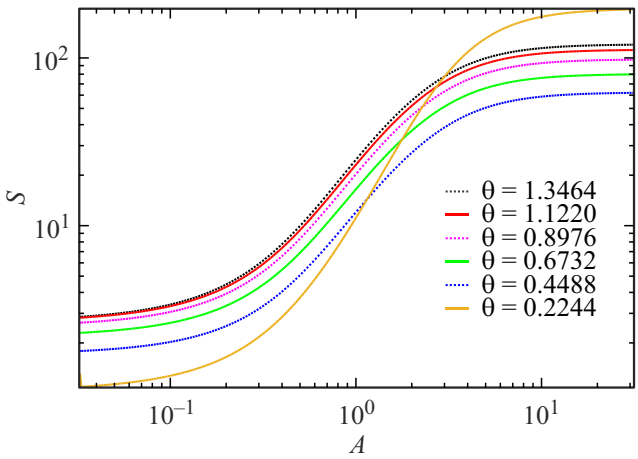

Figure 4. Scattered emission intensity vs. pumping wave heterogeneity A at different scattering angles θ; pumping wave parameters $G = 1$, $P = 5$; scattering region parameters $L_{1A}/L_2 = L_{1B}/L_2 = 2.5$.

with the experimental data. The difference shows that additional factors are present in the experiments which influence BSS and have not been included in the theoretical model.

Conclusions

The study was focused on the BSS process in a 2D localized and heterogeneous pumping wave field at an arbitrary scattering angle using reduced equations for the scattered and sound wave amplitudes in plasma. Accurate solutions have been obtained for spatial distribution of the scattered wave amplitude and scattered emission intensity. The equations have been written in such a way as to ensure the most obvious comparison with an infinite medium.

1. It has been found that, when the instability threshold was exceeded to a great extent, the highest scattering occurred in the direction along which the wave interaction region has the largest size. In particular, for the scattering region extended in direction $0X$, the most intense scattering shall take place in this direction.

2. When the scattered electromagnetic wave amplification region size is limited by heterogeneity, scattering takes place in direction $0X$ when the instability threshold is exceeded to a great extent, provided that the characteristic heterogeneity size is larger than the lateral dimension of the interaction region. Otherwise, scattering takes place in lateral direction (lower curves in Fig. 3, *b*).

3. When the instability threshold is exceeded to a low extent and the electromagnetic wave amplification in the interaction region is comparable with damping in the neighborhood, the scattering emission dependence becomes more complicated.

4. Comparison of the calculations of scattered emission intensity at BSS using the obtained equations with the experimental data has demonstrated their qualitative agreement.

Conflict of interest

The authors declare that they have no conflict of interest.

References

[1] N.M. Kroll. J. Appl. Phys., **36** (1), 34 (1965). DOI: 10.1063/1.1713918
[2] D.L. Bobroff, H.A. Haus. J. Appl. Phys., **38** (1), 390 (1967). DOI: 10.1063/1.1708986
[3] L.M. Gorbunov. Sov. Phys: Zh. Tekh. Fiz., **47** (1), 36 (1977).
[4] A.D. Piliya. Zh. Eksp. Teor. Fiz., **64** (4), 629 (1973).
[5] L.M. Gorbunov, D.K. Solikhov. Sov. Phys.: Fiz. Plasmy, **10** (4), 824 (1984).
[6] D.K. Solikhov. Radiophysics and Quantum Electronics, **27** (1), 25 (1984). DOI: 10.1007/BF02120939.
[7] D.K. Solikhov, K.N. Ovchinnikov. Bulletin of the Lebedev Physics Institute, **37** (10), 3 (2010). DOI: 10.3103/S1068335610100015.
[8] D.K. Solikhov, S.A. Dvinin. Plasma Physics Reports, **42** (6), 576 (2016). DOI: 10.1134/S1063780X16060076.
[9] D. Pesme, G. Laval, R. Pellat. Phys. Rev. Lett., **31** (4), 203 (1973). DOI: 10.1103/PhysRevLett.31.203
[10] D.F. DuBois, D.W. Forslund, E.A. Williams. Phys. Rev. Lett., **33** (17), 1013 (1974). DOI: 10.1103/PhysRevLett.33.1013
[11] S. Iha, S. Srivastava. Phys. Rev. A, **11** (1) 378 (1975). DOI: 10.1103/PhysRevA.11.378
[12] F.W. Chambers, A. Bers. Phys. Fluids, **20** (3), 466 (1977). DOI: 10.1063/1.861884
[13] V. Fuchs, C. Beaudry. Phys. Fluids, **21** (2), 280 (1978). DOI: 10.1063/1.862203
[14] Z. Toroker, V.M. Malkin, N.Z. Fish. Physics of Plasmas, **21** (11), 113110 (2014). DOI: 10.1063/1.4902362
[15] L.M. Gorbunov. UFN, **109** (4), 631 (1973) (in Russian). DOI: 10.3367/UFNr.0109.197304a.0631 [L.M. Gorbunov Uspekhi Fizicheskikh Nauk (Physics-Uspekhi), **16** (2), 217 (1973). DOI: 10.1070/PU1973v016n02ABEH005166].
[16] S.A. Dvinin, D.K. Solikhov, Sh.S. Nurulkhakov. Opt. i spektr., **128** (1), 98 (2020) (in Russian). DOI: 10.21883/OS.2020.01.48844.271-19 [S.A. Dvinin, D.K. Solilhov, Sh.S. Nurulhakov. Opt. Spectrosc., **128** (1), 94 (2020). DOI: 10.1134/S0030400X20010075].
[17] A. Bers. In: *Handbook of Plasma Physics. Vol. 2*, ed. by A.A. Galeev and R.N. Sudan, (North-Holland Publishing Company, 1983), p. 451–514.
[18] S.A. Dvinin, D.K. Solikhov, D.U. Hobilov. In: *XLVIII Zvenigorod Conference on Plasma Physics and Controlled Fusion. Zvenigorod, 15–19 March 2021*. DOI: 10.34854/ICPAF.2021.48.1.154.
[19] D.K. Solikhov, S.A. Dvinin, D.U. Khobilov. Russian Physics J., **62** (12), 42 (2019). DOI: 10.1007/s11182-020-01967-y.
[20] A.A. Offenberger, M.R. Cerveman, A.M. Yam, A.W. Pasternak. J. Appl. Phys., **47** (4), 1451 (1976). DOI: 10.1063/1.322806
[21] A. Ng, L. Pitt, D. Salzmann, A.A. Offenberger. Phys. Rev. Lett., **42** (5), 307 (1979). DOI: 10.1103/PhysRevLett.42.307